NASA DEVELOP National Program
Virginia – Langley
Summer 2022

Chile Wildfires

Utilizing NASA and NOAA Earth Observations to Determine Lightning-ignited Wildfire Risks in Central Chile

DEVELOP Technical Report
Final – Aug 10th, 2022

Christopher Matechik (Project Lead)
Jennifer Ruiz
Reuben Alter
Stephen Sene

Advisors:
Kenton Ross, NASA Langley Research Center (Science Advisor)
Kristopher Bedka, NASA Langley Research Center (Science Advisor)

1. Abstract

In recent years, Central Chile has experienced wildfires of increasing frequency and intensity which threaten natural resources and communities. The Corporación Nacional Forestal (CONAF) responds to wildfires caused by a variety of ignitions, including lightning, but it is difficult to determine the prevalence of lightning-ignited wildfires based solely on ground observations. In collaboration with CONAF and the Embassy of Chile, Agricultural Office, the team used Earth observations to map coincidence of lightning strikes and wildfire ignitions. The Active Fire Product of Suomi NPP Visible Infrared Imaging Radiometer Suite (VIIRS) identified wildfires as thermal anomalies, which the team compared to the lightning events detected by NOAA's GOES-16 Geostationary Lightning Mapper (GLM). Next, the team mapped lightning strike frequency and lightning related wildfires across the study area. Finally, the team calculated and mapped a relative estimate of lightning-ignited wildfire vulnerability across the year, fire season (December – March), and off-season (April – November) by summing the following factors: lightning frequency, the Normalized Difference Moisture Index (NDMI) and land surface temperature (LST). These risks were then weighted by fuel availability. Preliminary analysis of the lightning fire relationship showed a spatiotemporal coincidence, primarily in the South-central region of study, near Temuco, and isolated areas on the Andean front. The team identified areas at risk of lightning-induced wildfires, predominantly in the northern third of the study area and along the Andean front. Adjusting the relative weight of risk factors and improving the lightning and fire coincidence map by clustering VIIRS thermal anomalies into fire events could reduce discrepancies and improve risk assessments for future work.

Key Terms
lightning, remote sensing, risk map, vegetation water content, fuel moisture

2. Introduction

2.1 Background Information

Wildfires in Central Chile have been increasing in frequency, and destructive capacity, threatening ecosystems and posing a significant risk to human populations (Úbeda & Sarricole, 2016). Specifically, wildfires destroy habitat, destabilize soils, release carbon, pollute water, destroy crops, harm livestock, destroy homes, cause respiratory distress by reducing air quality, and occasionally cause human mortality (Úbeda & Sarricole, 2016). The majority of wildfires in Chile are attributed to anthropogenic causes, while only 0.2 percent are attributed to natural ignition, in the form of lightning strikes or volcanoes (CONAF, 2015). However, recent studies have suggested that the proportion of lightning-ignited wildfires is underestimated. For example, Veblen et al. (1995) noted the presence of fire-adapted tree species in southern South America, suggesting the occurrence of natural fires. Regardless, lightning-ignited wildfires are still a significant concern because they tend to burn more acreage than anthropogenic fires despite being less frequent (Úbeda & Sarricole, 2016). The Corporación Nacional Forestal (CONAF) responds to wildfires in Chile and wants to understand the relationship between lightning frequency and wildfire prevalence, and use that relationship to predict lightning-ignited wildfire risks. CONAF is especially interested in central Chile because it is fire prone and encompasses major urban areas adjacent to remote, uninhabited areas.

The study area (Figure 1) stretches between Chile's Eastern and Western borders – the Andes Mountains and the Pacific Ocean, respectively – and extends from Los Vilos in the north to Rio Negro in the south. The area is highly populated, housing the cities of Santiago, Valparaiso, and others, but also contains large amounts of agro-grazing-forestry land use (Úbeda & Sarricole, 2016). Containing several large population centers, this area of Central Chile is experiencing increases in wildland urban interface, or areas where human development overlaps with fire-prone natural spaces (Garfias et al., 2012). This area has a Mediterranean climate, which is characterized by warm dry summers and sclerophyllous plant life (Castillo et al., 2020). Silviculture operations are actively replacing native species with pyrophytic invasives – primarily Monterey Pine (*Pinus radiata)* and Blue Gum Eucalyptus (*Eucalyptus globulus)* (Villacrés et al., 2019). Climate change is expected to decrease precipitation throughout Chile (Fuenzalida et al., 2006) resulting in an increase in wildfire frequency and burned acreage (González et al., 2011). Villacres et al. (2019) stated that understanding wildfire risks is crucial to allocate management efforts and suggested using remote sensing as an efficient method to assess risk. The study period ranged from March 1, 2018, through February 28, 2022. This was determined by availability of lightning occurrence data and the need to use a temporal range that represented more recent climatic conditions, as both the literature and CONAF have noted that fire regimes are changing with climate change (Úbeda & Sarricole, 2016).

Figure 1. Central Chile study area with an inset showing the location in relation to the rest of Chile and South America.

2.2 Project Partners & Objectives

CONAF is responsible for sustainable management of Chile's forests via planning for, preventing, detecting, monitoring, and suppressing wildfires in Chile's forested and protected areas. The Embassy of Chile, Agricultural Office, serves as a liaison between Chilean and United States government offices and facilitates partnerships between NASA and Chile, with the goal of using remote sensing technology to improve wildfire management. The partners aim to protect Chilean ecosystems, human population, and critical resources for economic stability and safety. CONAF believes that lightning is a significant contributor to wildfires in central Chile, yet the relationship between lightning occurrence and wildfire ignitions is not well known. Similarly, the relative risk of lightning-ignited wildfires occurring across the study area is unknown.

To help the partners meet their goals, this project sought to visually determine the spatial relationship between lightning occurrence and wildfires, and to create a map of lightning-ignited wildfire relative risk. Specifically, the team (1) mapped past lightning strikes and historic wildfires from March 2018 through February 2022, (2) analyzed the spatiotemporal relationship between lightning strikes density and wildfire ignition, (3) calculated and mapped the Normalized Difference Moisture Index (NDMI), and (4) calculated and mapped the relative risk of

lightning-ignited wildfire risk. The maps created as part of these objectives will provide the partners with a visual understanding of where lightning-ignited wildfires can be expected to occur. CONAF can use the information to allocate fire detection, prevention, and suppression resources.

3. Methodology

3.1 Data Acquisition

The team downloaded all data for the entire study period from March 1, 2018 – when lightning data first became reliably available – through February 28, 2022. Additionally, the team subset all data products into the fire season, December through March, and the off season, April through November, in order to examine seasonal trends. Grouping into fire and off season was either performed prior to downloading, or during data processing, depending on the data.

The team acquired the National Oceanic and Atmospheric Administration (NOAA) GOES-16 Geostationary Lightning Mapper (GLM) L2 data from the NOAA Amazon Web Services S3 data archive using an Amazon Web Services Command Line Interface direct copy script.

The team accessed Active Fire Product (AFP) data from Suomi NPP VIIRS via NASA's Fire Information for Resource Management System (FIRMS) as two separate data sets. The archive data contained thermal anomaly points that occurred from the beginning of our study period through December 31, 2021. The near real time (NRT) data set contained thermal anomaly points that occurred from January 1, 2022, through the end of our study period. The team worked under the assumption that thermal anomalies represented fires, so the two terms can be considered interchangeable hereafter. The team acquired Suomi NPP VIIRS Land Surface Temperature and Emissivity (LST) data from USGS and NASA Earthdata as a collection of hierarchal data format (HDF) files. The data were filtered to the study area and time period prior to downloading using the Earthdata graphical user interface. The Earthdata portal automatically generated a Git script that the team used to download the data in bulk. Seasonal subsets were downloaded using the same procedures.

The team acquired collection 2, tier 1, level 2 Landsat 8 Operational Land Imager (OLI) data for the entire study period via GEE at a spatial resolution of 30 square meter pixels (Table 1). The team masked by removing all cloud, dilated cloud, and cloud shadow pixels and then median reduced prior to downloading. The same procedures were used to produce seasonal subsets.

Table 1
Earth observations data used in this project, organized by their platform and sensor.

Platform & Sensor	Parameters	Dataset	Use	Date Range
GOES-16 GLM	Total Lightning	GLM-L2-LCFA	Total Lightning was used to identify lightning events across central	March 1, 2018, through February

			Chile	28, 2022
Suomi NPP VIIRS	AFP LST	VNP14A1 VNP 21A1Dv0 01	AFP was used to create layers of fires for use in the lightning map and fire risk map. LST was used as a risk factor for wildfire ignition, to identify warming trends among years, and to determine the most active fire season.	March 1, 2018, through February 28, 2022 March 1, 2018, through February 28, 2022
Landsat 8 OLI	NDMI	Collection 2 Level 1 Surface Reflectance	NDMI was used to calculate vegetation moisture, identify dry areas for the moisture map, and serve as a factor for wildfire risk.	March 1, 2018 through February 28, 2022

3.2 Data Processing

The team took the GLM lightning data, in netCDF4 form, and converted them into a file structure with lower data requirements, as the raw data were collected at a 20 second period for four years. Removing the majority of variables in the data, save location, strike energy, and a unique identifier allowed for easier processing later in the methodology. The team only utilized data on the flash scale, as utilizing event and group from the GLM data structure would have proved unwieldly and the added precision from lower tier data would have been lost when brought to the broader spatial extent of this project. From there, the team divided lightning into fire season, off season, and year-round files, and uploaded them into ArcGIS Pro 2.9, where the team reprojected and clipped them to fit the study area.

The team imported the two AFP datasets into ArcGIS Pro 2.9, merged them into one feature class, and then clipped them to the study area using. Subsets for the fire season and off season were created by selecting the appropriate months using the select by attributes tool and then exporting each selection as a separate feature class. LST data for the entire study period and each season were imported into separate mosaic datasets in ArcGIS Pro 2.9, median reduced, and then clipped to the study area. GEE exported the Landsat 8 data in multiple TIFFS, so the team imported the files into ArcGIS Pro 2.9, mosaiced the images into one TIFF using the mosaic raster tool, and then clipped the TIFF to the study area. Next, the

NDMI was calculated using Equation 1 as derived from the U.S. Geological Survey (USGS), below:

$$NDMI = \frac{NIR - SWIR}{NIR + SWIR} \quad (1)$$

Next, the team clipped all layers to a fuel mask provided by CONAF indicating which areas contain enough fuel quantity and continuity to burn. Additionally, In ArcGIS Pro 2.9, the team converted the fuel mask layer into a raster representing the proportion of fuel laden area in fishnet cells. First, the team used the create fishnet tool in ArcGIS Pro 2.9 to create an 8km-by-8km square grid over the study area. The team selected this cell size to accommodate the uncertainty of the GLM data. The GLM sensor has an uncertainty range of ± 8 kilometers from the nadir, or the point directly below the satellite within the given reference system. Thus, an 8km grid allows for uncertainty within a range of one cell in any direction from the location of actual strike, leading to less inaccuracy as compared to the hypothetical smaller grid. Next, the team used the intersect tool to create polygons of fuel-laden area within each cell, and then the dissolve tool (with the fishnet ID as the dissolve parameter) to merge disjunct polygons within the same cell. The Shape_Area attribute of the dissolved polygons layer was joined back to the original fishnet layer, yielding an attribute table with fields containing the total area and the fuel laden area for each fishnet cell. Finally, the calculate fields tool was used to calculate the proportion of each cell that was fuel laden according to equation 2.

$$\frac{\text{Fuel Laden Area}}{\text{Total Cell Area}} \quad (2)$$

3.3 Data Analysis

First, the team created a program that creates a spatiotemporal buffer around each VIIRS AFP point and counts the number of lightning strikes within said buffer. This serves as a non-causal analysis system for understanding where, and when, lightning strikes are in the same general area as new fires. For the scope of the project, that was as close as the team could get to understanding coincidental lightning strikes and wildfires.

Next the team used a fishnet analysis to calculate relative lightning ignited wildfire risks using the following factors: lightning frequency, LST, NDMI, and fuel (Figure 2). The team summarized each factor by calculating a value for each cell using the same 8km by 8km fishnet used to calculate percent fuel. Lightning strikes were represented by point data, so the team tallied the number of strikes per grid cell using a spatial join and then standardized the count to counts per month by dividing by the number of months in the seasonal data set (12 for all seasons, 4 for fire season, 8 for off season). LST and NDMI were represented by raster data, so the median pixel value in each grid cell was calculated using the zonal statistics tool. The fishnet LST means, NDMI means, and lightning strike frequencies were sorted into broadly ranked risk categories ranging from 1-5 using the reclassify tool and the reclassification schemes shown in Table 2. Lightning risk ranks

(Figure 3) were dominated by low-risk rank areas, with small areas of high-risk ranks along the Andean front, which were highest during fire season. The team calculated the cumulative risk by summing the individual risk ranks for LST, NDMI, and lightning strikes, and then multiplying that value by the percent of fuel laden area in that cell (Figure 3)

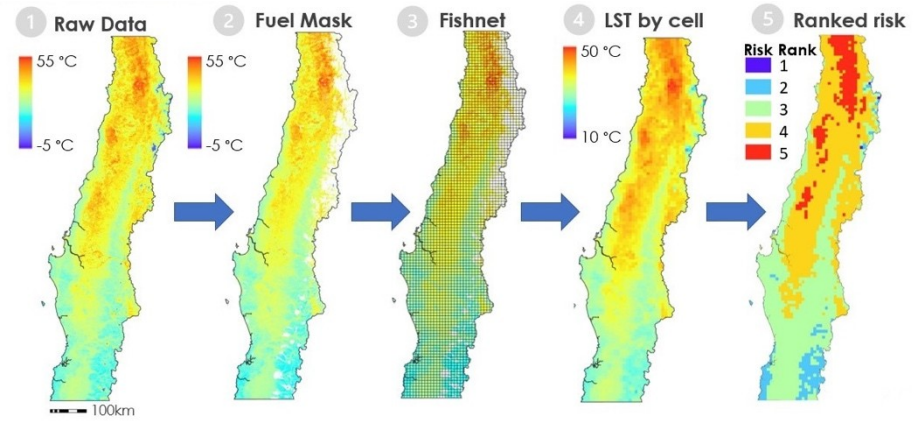

Figure 2. A schematic of the fishnet analysis used to calculate the relative risk ranks across the study area. This example depicts risk ranks for LST during the fire season, but the methodology was for all seasonal periods and for NDMI and lightning frequency data.

Table 2
Risk rank scales for each GLM, NDMI, and LST risk.

GLM Rank	Lower Strike Value	Upper Strike Value
1	0	5.7
2	5.7	15.9
3	15.9	34.4
4	34.4	66.3
5	66.3	131
NDMI Ranks	Lower NDMI Value	Upper NDMI Value
1	162.6	597
2	111.3	162.7
3	55.7	111.3

4	-1.9	55.7
5	-107	-1.9
LST Ranks	Lower LST (°C)	Upper LST (°C)
1	-14	0.5
2	0.5	13
3	13	25.5
4	25.5	38
5	38	50.6

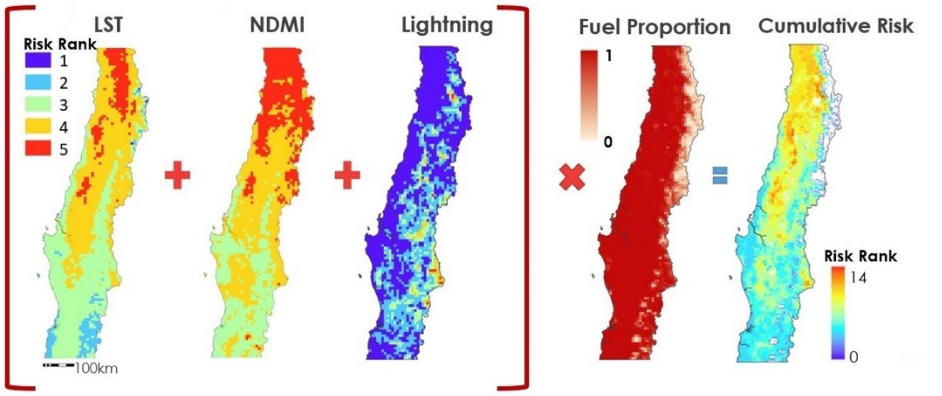

Figure 3. A schematic of cumulative risk rank calculation for fire season. The same methodology was also applied to off season and all seasons.

4. Results & Discussion

The results showed a high frequency of lightning strikes (Figure 4), VIIRS thermal anomaly (fire points) frequencies (Figure 5), and spatiotemporally filtered VIIRS thermal anomaly (fire points) (Figure 6) along the Andean front. However, thermal anomalies (Figure 5) and filtered thermal anomalies (Figure 6) were also prevalent in the south-central zone of the study area, where lightning strikes were not quite as frequent (Figure 4).

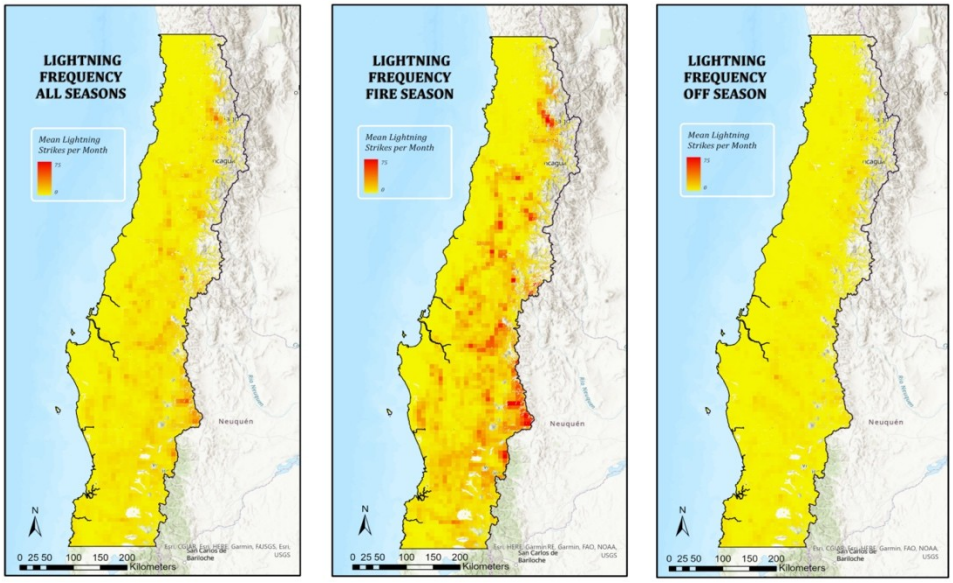

Figure 4. Average lightning frequency per month across Central Chile for all seasons, fire season, and off season at an 8km-by-8km resolution. Data were standardized to the average lightning strike frequency per month to enable comparison among seasons. Data were masked by fuel presence.

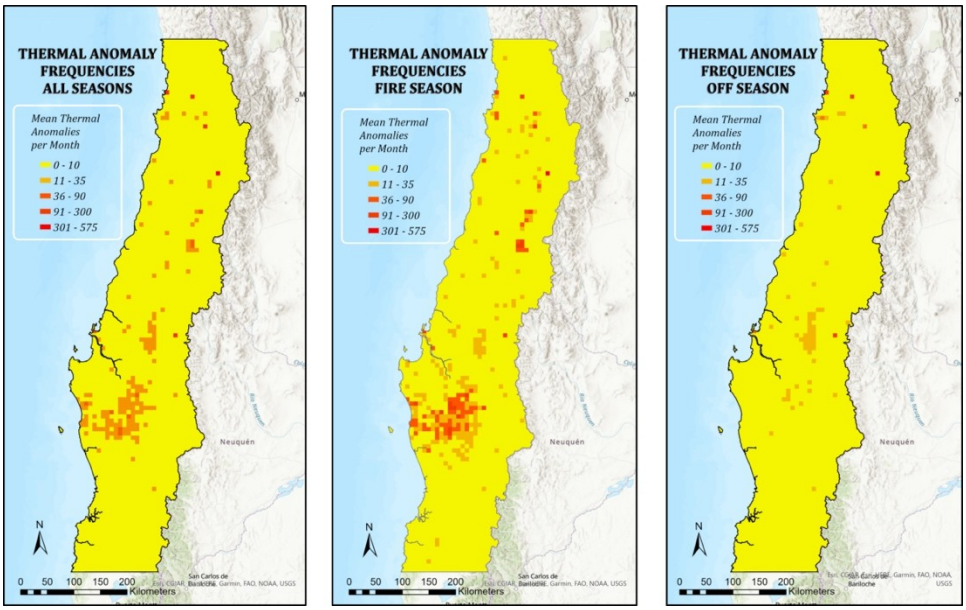

Figure 5. Average VIIRS thermal anomaly frequency per month across central Chile for all seasons, fire season, and off season at an 8km-by-8km resolution. Data were standardized to the average number of thermal anomalies per month to enable comparison among seasons.

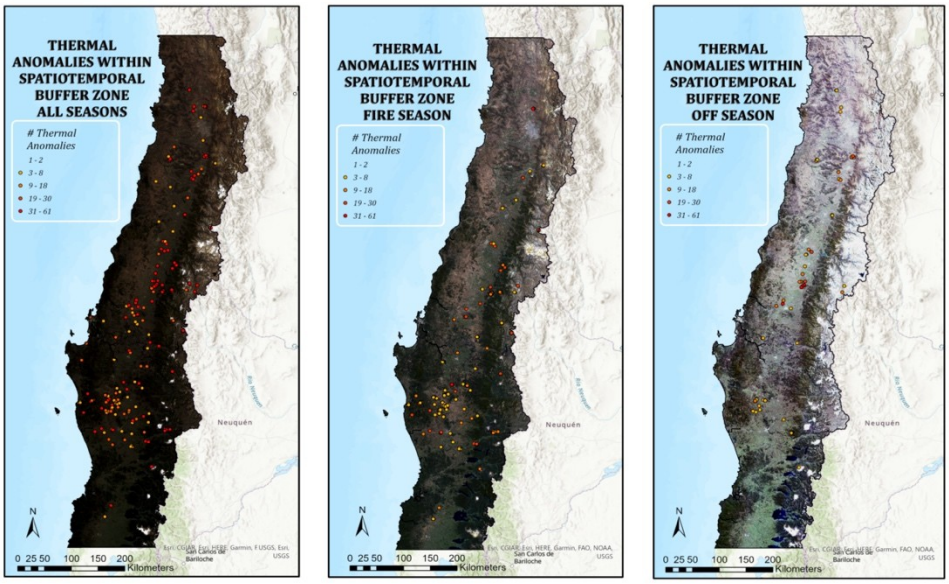

Figure 6. VIIRS thermal anomalies that were coincidental with GLM detected lightning strikes. Thermal anomalies were considered coincidental if the lightning strike occurred within a 4km radius and 3 days of an anomaly. Data were masked by fuel presence.

Lightning frequency (Figure 4) and risk ranks (Figure 7) were highest along the Andean Front, whereas LST (Figure 8) and NDMI (Figure 9) and their respective risk ranks (Figures 10 and 11; Table 2) were both highest in the northern third of the study area where it is known to be arid. All risk factors were greatest during the fire season. NDMI had the least amount of variation among seasons, only slightly increasing in risk from fire season to off season.

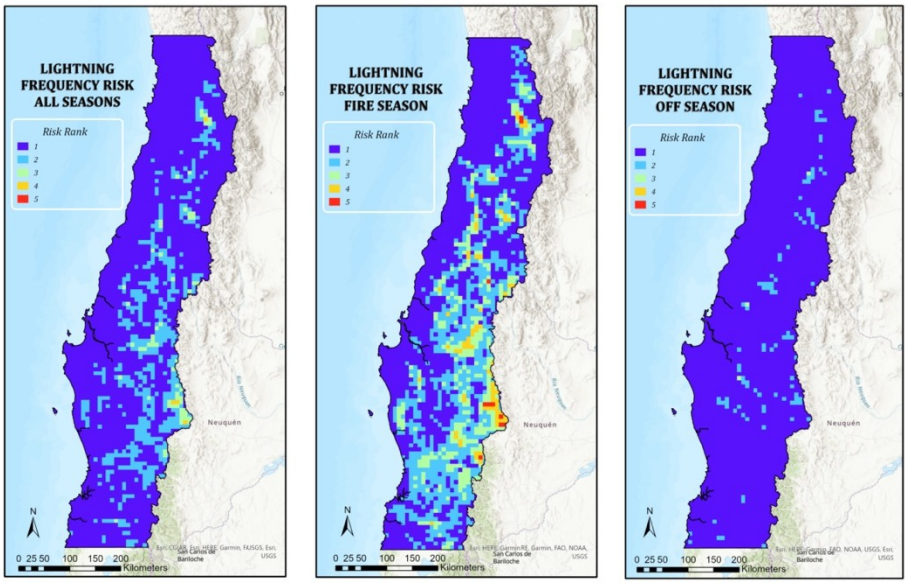

Figure 7. Lightning strike risk, derived from monthly strike frequency, for all seasons, fire season, and off season at an 8km-by-8km resolution.

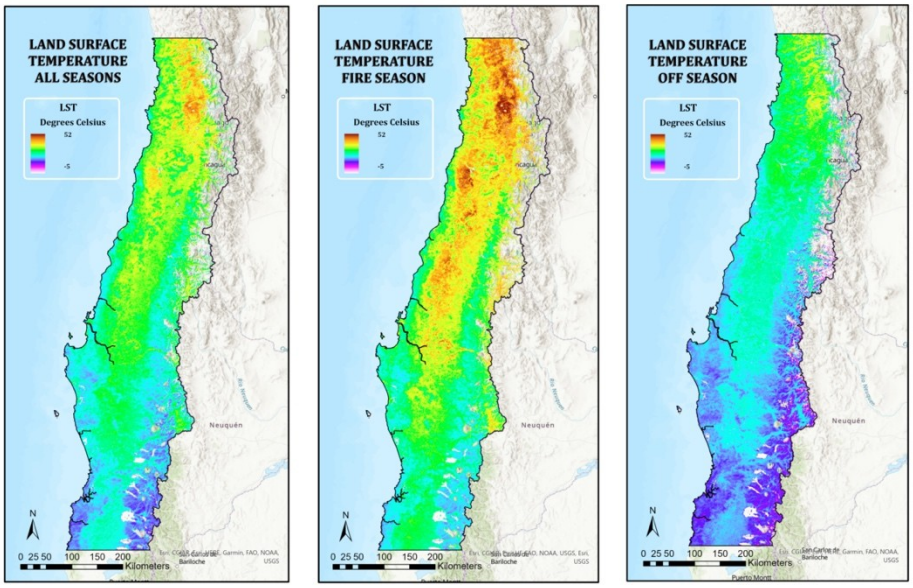

Figure 8. Median LST, at a 1km spatial grain, in degrees Celsius for all seasons, fire season, and off season. Data were masked by fuel presence.

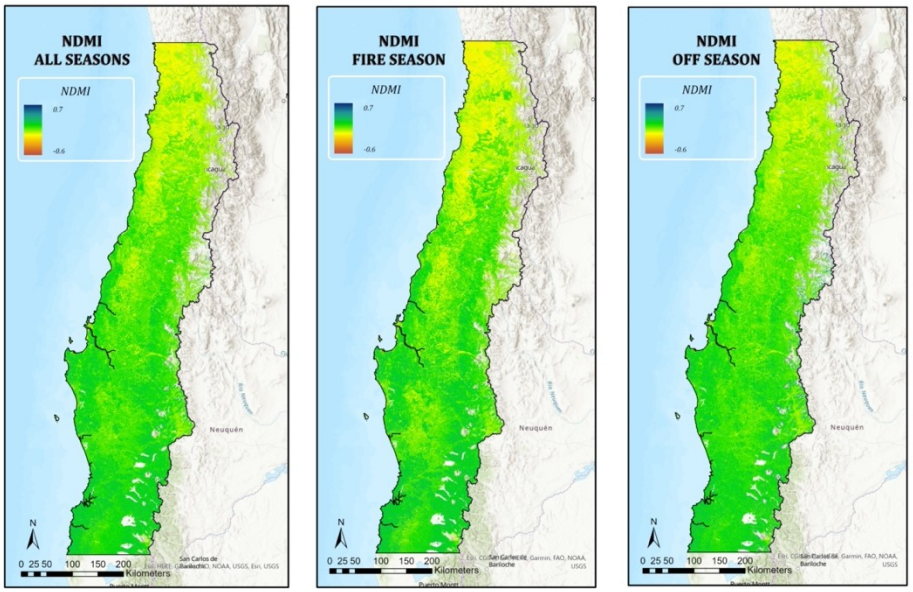

Figure 9. Median NDMI, at a 30-meter spatial grain, in degrees Celsius for all seasons, fire season, and off season. Data were masked by fuel presence.

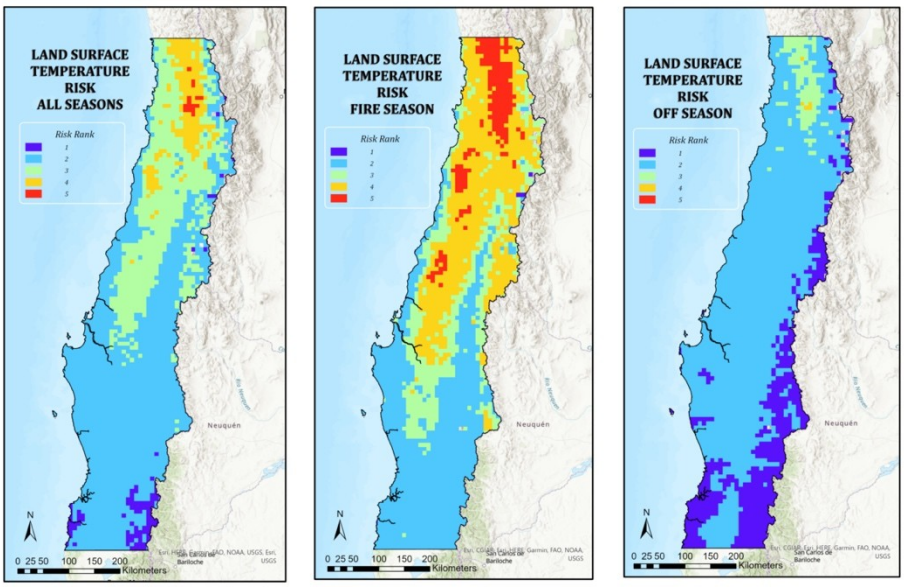

Figure 10. LST risk, derived from VIIRS LST data, for all seasons, fire season, and off season at an 8km-by-8km resolution.

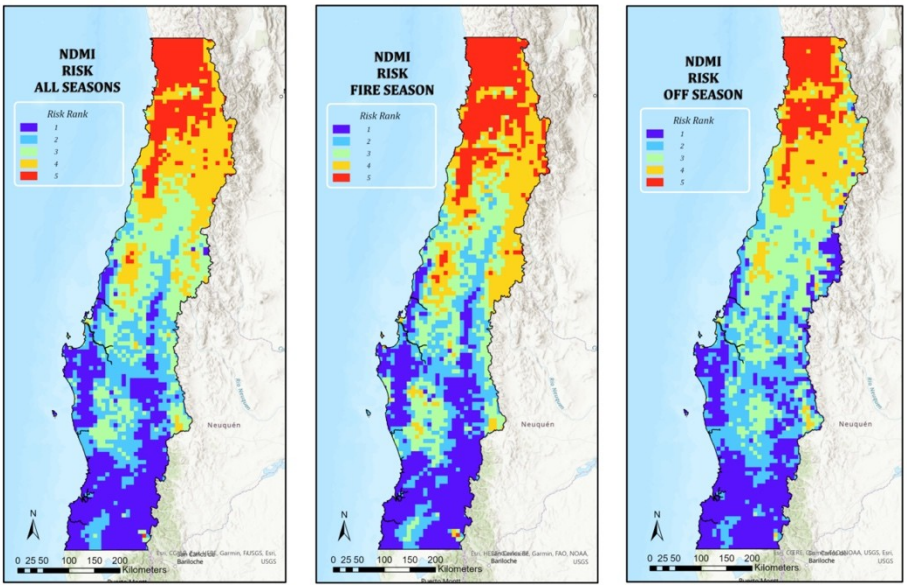

Figure 11. NDMI risk, derived from Landsat8 OLI surface reflectance data, for all seasons, fire season, and off season at an 8km-by-8km resolution.

The cumulative wildfire risk (Figure 12) was greatest in the northern third of the study area during the fire season and showed similar patterns to the LST and NDMI risk maps. During fire season, there was a slight increase in cumulative risk in the south-central part of the study area where thermal anomalies related to wildfires occurred.

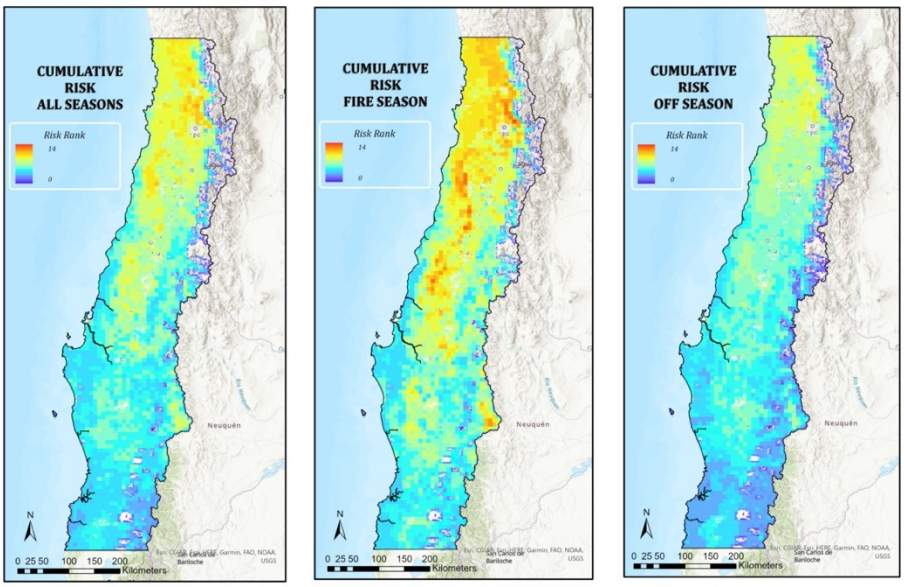

Figure 12. Cumulative wildfire risk as a function of lightning frequency, LST, NDMI, and fuel for all seasons, fire season, and off season at an 8km-by-8km resolution.

4.1 Analysis of Results

A visual assessment of figures 4, 5, and 6 shows a discrepancy between where lightning strikes occur, primarily along the Andean front, and where both lightning associated and non-lightning-associated thermal anomalies (i.e., fires) occur, in the south-central part of the study area. There were more thermal anomalies associated with lightning strikes in the south-central study area (Figure 6), but also more thermal anomalies overall (Figure 5), so it is unclear if lightning is more likely to result in ignitions in this area, or if there are just more fires (natural and anthropogenic) overall. The team was unable to determine if thermal anomalies associated with lightning strikes were causal with fire. Lightning strike frequencies were high along the Andean Front (Figure 4) where the team observed relatively high numbers of lightning-associated thermal anomalies, but qualitative inspection of these points and conversations with CONAF staff revealed that many of them are known to be caused by geothermal features, mining, or agricultural activities. Thus, there are actually fewer fires than shown along the Andean Front where lightning strike frequencies are highest. This suggests that lightning frequency may not be the driving factor of lightning-ignited wildfire. For example, less continuous vegetation in alpine zones may limit fire spread or start. Additionally, the team did not include active precipitation in the temporal filter, which may be another reason for a lack of fires in the Andes – there may be more precipitation and fewer dry strikes.

The cumulative risk map is biased to the northern third of the study area (Figure 12) when in reality wildfires related to lightning strikes (Figure 6) are more likely to occur in the south-central part of the study area. The cumulative risk maps are similar to the LST and NDMI risk maps, suggesting that these factors carry too much weight in the cumulative risk calculation. LST and NDMI are both related to aridity, so it is possible that including the two factors without adjusting their

weights was redundant. However, the methodology used to derive the cumulative risk map may still prove useful to the partners since the relative weights of each factor can be adjusted. Additionally, the risk ranks for each factor could be improved by using risk ranks based on experimentally determined thresholds, but the team was unable to find appropriate thresholds in the literature.

4.2 Future Work

Although the cumulative risk maps are not congruent with observed fires and CONAF's *in situ* observations, future work refining the risk calculations could make the risk map operationally applicable. Specifically, refinement should include improved risk weighting, inclusion of relevant risk factors, and more accurate spatiotemporal filtration. The team assumed that all factors were weighted equally because the relative influence of factors on wildfire ignitions was unknown. One method of improving risk weights is creating multiple versions of the model with different factor weights and then comparing the output to observed thermal anomalies. The model could also be improved by including additional factors that have been shown to influence wildfire in other areas such as elevation, slope, aspect, and vegetation type. Spatiotemporal filtration would require a tool for clustering VIIRS AFP thermal anomaly data, while also screening it for manmade anomalies, such as mines, and non-fire natural anomalies, such as volcanoes. This would preferably be a tool that works in near real-time as well as for historic data. The clustering would need to find a likely point of origin, along with the associated time. From there, origin points could be correlated with spatiotemporally preceding lightning strikes and a wildfire-lightning connection could be built, or at least started. This work would need to be done using a larger spatial extent, or study area, than that of this project, and in order to have enough data, the extent would need significant extension.

5. Conclusions

The team provided the partners with a preliminary lightning ignited wildfire risk map. Understanding risk throughout the study area will allow partners to anticipate fires and allocate resources accordingly. The risk calculations need some improvement but the framework for the model is already established so the aforementioned improvements would be easy to implement. Additionally, the team provided CONAF with lightning, LST, NDMI, and thermal anomaly datasets that they can use for creating their own fire risk analyses or other purposes related to silviculture. The team hopes that the data will provide substantial insight to the partners and will act as a valuable tool that can provide further protection to communities located in areas of high lightning-ignited wildfire risk. With the work that the team has provided, our partners are better informed of risk in their management areas and can thus hopefully improve wildfire management techniques in a manner non-intrusive to their current practices. This can help lower negative outcomes from wildfires that communities and the Chilean economy faces.

In the data analysis, a low number of strikes preceded fire when run in the spatiotemporal buffer, with only a few hundred anomalous points in the study period showing said pattern. Because of this finding, the team believes that lightning could be as low an ignition risk as previous literature stated (Menezes et al. 2022). More work must be done to conclude this in a quantitative way.

6. Acknowledgments

The team gives thanks to Dr. Kenton Ross and Kristopher Bedka for their guidance as scientific advisors for the project. The team gratefully acknowledges the cooperation, understanding, and guidance their partners at CONAF and the Chilean Embassy showed them throughout the study. Lastly, the team gives many thanks to Adriana Le Compte for her support, insight, and mentorship throughout the term as their node fellow.

DigitalGlobe/Maxar data were provided by NASA's Commercial Archive Data for NASA investigators (cad4nasa.gsfc.nasa.gov) under the National Geospatial-Intelligence Agency's NextView license agreement.

This material is based upon work supported by NASA through contract NNL16AA05C.

7. Glossary

Earth observations – Satellites and sensors that collect information about the Earth's physical, chemical, and biological systems over space and time
AFP – Active Fire Product of the Suomi NPP VIIRS satellite.
GLM – Geostationary Lightning Mapper sensor on the NOAA GOES-16 (previously GOES-R) satellite.
NDMI – Normalized Difference Moisture Index; an index representing the relative moisture of vegetation.
Sclerophyllous – Refers to plants adapted to long periods of dryness and heat.
VIIRS – Visible Infrared Imaging Radiometer Suite sensors on the Suomi National Polar Orbiting Partnership (NPP) satellite.
GOES-16 – Geostationary Operational Environmental Satellite 16. NOAA run satellite that houses the Western hemisphere GLM.

8. References

Castillo S, M., Plaza V, Á, & Garfias S, R. (2020). A recent review of fire behavior and fire effects on native vegetation in Central Chile. Global Ecology and Conservation, 24, e01210. https://doi.org/10.1016/j.gecco.2020.e01210

CONAF, *Forest Fire Detection.* https://www.conaf.cl/incendios-forestales/combate-de-incendios-forestales/deteccion-de-incendios-forestales/

Fuenzalida, H., Falvey, M., Rojas, M., Aceituno, P., & Garreaud, R. (2006). Estudio de la variabilidad climática en Chile para el siglo XXI. *Informe para CONAMA*.

Garfias S., R., Castillo S., M., Ruiz G., F., Julio A., G., Quintanilla P., V., & Antúnez G., J. (2012). Caracterización socioeconómica de la población en áreas de riesgo de incendios forestales. Estudio de caso. Interfaz urbano-forestal, provincia de Valparaíso. Chile central. *Territorium,* (19), 101-109. https://doi.org/10.14195/1647-7723_19_12

GOES-R Algorithm Working Group and GOES-R Series Program, (2018): NOAA GOES-R Series Geostationary Lightning Mapper (GLM) Level 2 Lightning Detection: Events, Groups, and Flashes (GLM-L2-LCFA). [Data set]. NOAA National Centers for Environmental Information. Accessed 2022-7-6 from https://doi.org/10.7289/V5KH0KK6

González, M. E., A. Lara, R. Urrutia, and J. Bosnich. 2011. Cambio climático y su impacto potencial en la ocurrencia de incendios forestales en la zona centro-sur de Chile (33°–42° S). *Bosque*, *32*(3), 215– 219. http://dx.doi.org/10.4067/S0717-92002011000300002

Hulley, G., Hook, S. (2018). VIIRS/NPP Land Surface Temperature and Emissivity Daily L3 Global 1km SIN Grid Day V001 [Data set]. NASA EOSDIS Land Processes DAAC. Accessed 2022-08-04 from https://doi.org/10.5067/VIIRS/VNP21A1D.001

Schroeder, W., Giglio, L. (2018). VIIRS/NPP Thermal Anomalies/Fire Daily L3 Global 1km SIN Grid V001 [Data set]. NASA EOSDIS Land Processes DAAC. Accessed 2022-08-04 from https://doi.org/10.5067/VIIRS/VNP14A1.001

Ubeda, X., & Sarricolea, P. (2016). Wildfires in Chile: A review. *Global and Planetary Change, 146*, 152-161. https://doi.org/10.1016/j.gloplacha.2016.10.004

Veblen, T., Burns, B., Kitzberger, T., Lara, A., & Villalba, R. (1995). The ecology of the conifers of southern South America. In N. Enright & R. Hill (Eds.), *Ecology of the Southern Conifers* (pp. 120-155). Melbourne University Press.

Villacrés, J., Arevalo-Ramirez, T., Fuentes, A., Reszka, P., & Auat Cheein, F. (2019). Foliar moisture content from the spectral signature for wildfire risk assessments in Valparaíso-Chile. *Sensors, 19*(24), 5475. https://doi.org/10.3390/s19245475

Úbeda, X., & Sarricole, P. (2016). Wildfires in Chile: A review. *Global and Planetary Change, 146*, 152-161. https://doi.org/10.1016/j.gloplacha.2016.10.004

U.S. Geological Survey Earth Resources Observations and Science Center. (2018). Landsat OLI Level-1 Surface Reflectance (SR). [Data set]. U.S. Geological Survey. https://doi.org/10.5066/F71835S6